

Modelling of Mechanical and Mechatronic Systems MMaMS 2014

Modeling of shock wave resistance in composite solidsMilan Žmindák^a, Zoran Pelagić^a^a*University of Žilina, Faculty of Mechanical Engineering, Department of Applied Mechanics, Univerzitná 1, 010 26 Žilina, Slovakia***Abstract**

The paper describes briefly the problem of elastic-plastic shock wave propagation in solids. Such waves originate by acting of explosion waves or by high velocity impact of solid parts on the structure. Computational simulations are applied to the elastic problem of propagation of waves in composite material reinforced by fibres. The fibres are supposed to be much stiffer than the matrix. The wave in such material is influenced by reflexion and refraction on the interface between fibres and the matrix and by the interaction of then waves. The wave is strongly damped in such composites in this way. The aim of this paper is to contribute better understanding and modelling of waves propagation using commercial software ABAQUS.

© 2014 Published by Elsevier Ltd. This is an open access article under the CC BY-NC-ND license (<http://creativecommons.org/licenses/by-nc-nd/3.0/>).

Peer-review under responsibility of organizing committee of the Modelling of Mechanical and Mechatronic Systems MMaMS 2014

Keywords: Wave propagation, fiber reinforced composite materials, finite element method

1. Introduction

In the recent years the interest about study of dynamical behavior in layered structures subjected to dynamical loadings [1]. Free vibrations [2] and transient dynamical analyses such as modal analyses found in the last thirty years the way towards practical applications in industry [3]. Analytical approaches that could give some insight into the behavior of structures started to be developed from the 17th century like Newton's theory of impact or the quasi-static impact theory, only to mention few. Although the development of analytical tools experienced a large progress through the years [4], they are only applicable for some basic problems. In the last decades, with the development of computers, numerical methods gained popularity for the solution of problems in the field of continuum mechanics. The finite element method (FEM), boundary element method (BEM) and the meshless methods like the Meshless Local Petrov - Galerkin (MLPG) [5, 6] are only few of the numerical tools which are used for the simulation

* Corresponding author. Tel.: +421 905847894
E-mail address: milan.zmindak@fstroj.uniza.sk

Nomenclature

σ_{ij}	stress tensor
S_{ij}	stress deviator tensor
p	pressure
δ_{ij}	kronecker delta
c	sound velocity
c_0	sound velocity in the material at zero pressure
S	experimentally determined parameter
$\mathbf{M}, \mathbf{C}, \mathbf{K}$	mass, damping and stiffness matrix
$\ddot{\mathbf{u}}, \dot{\mathbf{u}}, \mathbf{u}$	acceleration, velocity, displacement vector
$\mathbf{F}^{\text{ext}}, \mathbf{F}^{\text{int}}$	vector of external, internal forces
ω_{max}	maximum natural frequency
c_w	wave speed

of wave propagation problems. Currently, for wave propagation modeling in composite structures at low and high speeds is used mainly FEM, BEM, Fast Multipole BEM, respectively, Finite Volume Method (FVM), meshless formulations and recently connection of FEM and element free based formulations. However, very effective methods appear to be Spectral finite element methods (SFEM) for the solution of specific problems [7, 8]. For the analysis of dynamical problems commercial program systems LS-DYNA, AUTODYN and PAM CRASH etc. are used in practice. The aim of this paper is to contribute better understanding and modelling of waves propagation using commercial software ABAQUS.

2. Governing equations

We will not present here all governing equations for shock wave propagation as it would contain basic relations of continuum mechanics, which can the reader find in textbook of continuum mechanics [9, 10]. These equations are used to describe:

- the kinematics of solid continuum, the equations which present relation between displacements and corresponding displacement gradient for finite displacements in material and spatial description, strain tensors for finite strain formulation, strain measures and strain rate tensors,
- material and spatial time derivatives of deformations, velocity and velocity gradients,
- corresponding stress measures,
- formulation of equilibrium,
- conservation equations (conservation of mass, momentum and energy),

Thermodynamic laws give:

- the first law – the conservation of total energy,
- the second law – change in entropy,
- thermodynamic potentials – internal energy, enthalpy, Helmholtz and Gibbs free energy.

Further, the constitutive equations, which have to be thermodynamically consistent, give the relation between stress and strain measures. Dynamic deformation processes, especially when shock wave formation is involved, are usually modelled by decomposed stress tensor. The decomposition splits the stress tensor into a stress deviator tensor S_{ij} and a spherical hydrostatic pressure $p\delta_{ij}$, as:

$$\sigma_{ij} = S_{ij} - p\delta_{ij} \quad (1)$$

The usefulness of the decomposition results from the needed nonlinear character of equations of state to describe shock waves. In general, a pure material can be solid, fluid and gas.

Subjecting a structure to impact loading (impulse-type forcing) leads to the propagation of waves in the structure as an effect of forces associated with volume deformation. The main wave forms in solids are [11]:

- Longitudinal waves (Fig.1a): the characteristic particle motion is of compressional or stretching character. The wave propagation direction is parallel to the particle motion.
- Shear waves (Fig.1b): are characterized by transverse particle movements to the propagating wave direction. After longitudinal waves, they are the second fastest waves propagating in a structure. Alternative forms of shear waves are *bending waves*, which occur in structures of finite bending stiffness.
- *Rayleigh waves* (Fig.1c) are waves have a characteristic elliptic movement of particles, the propagation direction is parallel to the particle motion.

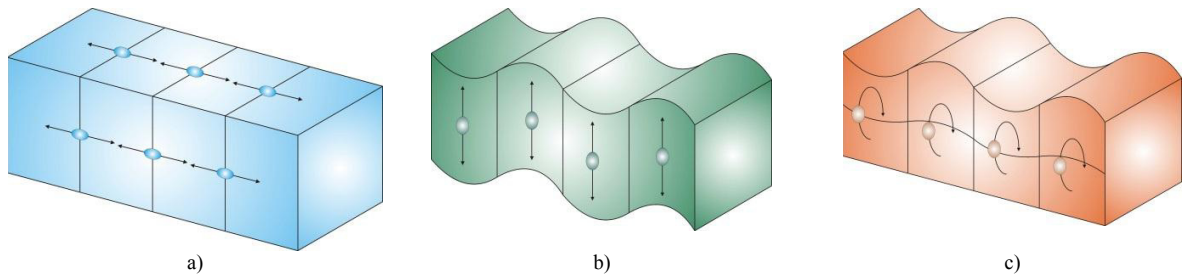


Fig. 1 Different wave types a) Longitudinal waves, b) Shear waves, c) Rayleigh waves

In structures of complicated form a complicated combination of all basic wave forms can be observed.. Characteristic properties of all shock waves are extremely short rise times as well as high pressure, density and temperature amplitudes.

Only if the load application is fast enough, the wave fronts of the faster packages keep up with the earlier wave fronts. The result is a steepened wave front and shorter rise times to higher pressures. Often, the wave components from the elastic regime are fast enough that a so called *elastic precursor* is formed. It is, however, also possible that even the elastic precursor is overtaken by very fast plastic waves. Whether or not this happens is only a matter of the load application speed and the achieved maximum pressure level.

For most materials the equation of state can be approximated as a linear relationship between the shock velocity and the particle velocity:

$$u_s = c_0 + S v_p \quad (2)$$

where S is experimentally determined parameter and c_0 is the sound velocity in the material at zero pressure. This is the case even up to shock velocities around twice the initial sound speed c_0 and shock pressures of order 100 GPa.

Recently the most successful method for modeling the dynamic response of a structure is FEM [12, 13]. The solution in the form of time integration can be, depending on the problem, accomplished via implicit or explicit methods [14, 15]. Although implicit methods are unconditionally stable (they are not dependent on the time step size), for wave propagation problems explicit methods have shown more suitability, cause they do not require stiffness, mass and damping matrix decomposition. The system of equations has the form

$$\mathbf{M}\ddot{\mathbf{u}}_{(t)} + \mathbf{C}\dot{\mathbf{u}}_{(t)} + \mathbf{K}\mathbf{u}_{(t)} = \mathbf{F}_{(t)}^{\text{ext}} \quad (3)$$

The solution of this system is carried out for each time step via the explicit central difference method. Here, the

acceleration in time t has the form

$$\ddot{\mathbf{u}}_{(t)} = \mathbf{M}^{-1}[\mathbf{F}_{(t)}^{\text{ext}} - (\mathbf{C}\dot{\mathbf{u}}_{(t)} + \mathbf{K}\mathbf{u}_{(t)})] = \mathbf{M}^{-1}[\mathbf{F}_{(t)}^{\text{ext}} - \mathbf{F}_{(t)}^{\text{int}}] \quad (4)$$

where $\mathbf{F}_t^{\text{ext}}$ is the vector of external forces and $\mathbf{F}_t^{\text{int}}$ is the vector of internal forces given as

$$\mathbf{F}_t^{\text{int}} = \sum \left(\int_{\Omega} (\mathbf{B}^T \sigma_n d\Omega + F^{hg}) \right) + F^{\text{cont}} \quad (5)$$

Velocities and accelerations have the form

$$2\Delta t \dot{\mathbf{u}}_{(t)} = \mathbf{u}_{(t+\Delta t)} - \mathbf{u}_{(t-\Delta t)} \quad (6)$$

$$\Delta t^2 \ddot{\mathbf{u}}_{(t)} = \mathbf{u}_{(t-\Delta t)} - 2\mathbf{u}_{(t)} + \mathbf{u}_{(t+\Delta t)} \quad (7)$$

The starting procedure has the form

$$\mathbf{u}_{(t-\Delta t)} = \mathbf{u}_{(0)} - \Delta t \dot{\mathbf{u}}_{(0)} + \frac{\Delta t^2}{2} \ddot{\mathbf{u}}_{(0)} \quad (8)$$

By applying zero initial conditions to the displacements and velocities, the starting procedure has the form

$$\ddot{\mathbf{u}}_{(t-\Delta t)} = \mathbf{M}^{-1} \mathbf{F}_{(0)}^{\text{ext}} \quad (9)$$

The stability of the central difference method depends on the length of the time step, which has to be divided into the shortest natural domains in the finite element mesh. The critical time step is computed by following relation [16, 17, 18].

$$\Delta t^{\text{critic}} = \frac{2}{\omega_{\max}} \quad (10)$$

where ω_{\max} is the maximum natural circular frequency. The calculation is based on Courant-Friedrichs - Lewy condition (CFL condition) for solving partial differential equations numerically by the method of finite differences

$$\omega_{\max} = 2 \frac{c_w}{l} \quad (11)$$

where c is the wave speed in the material and l is the characteristic length. By substitution (11) into (10) we obtain relation for critical time step

$$\Delta t = \frac{l}{c_w} \quad (12)$$

where Δt is time required for wave propagation in a rod with length l .

3. Computational results

In following example the composite material with modulus of elasticity and density equal to 210 GPa and 7830 kg m⁻³, respectively, is reinforced by straight fibres regularly distributed parallel to the upper surface (see Fig. 2). The modulus of elasticity of fibres is 100 times larger than that of the matrix. The loading of the material is perpendicular to the surface and it is increasing from zero to 0.0315 GPa in 0.05 μs and decreasing back to zero in same time. In order to describe the stress behaviour of a FRM, the material is modelled as a Representative Volume Element (RVE). This element describes the homogenous behaviour of the two phases, matrix and fiber, inside the RVE. Simulations are carried out with fibers with different diameters and volume fraction of fibers. We assume perfect adhesion between the fibers and matrix. It is a 2D problem (plain stress, $\nu=1$) and computational simulations were performed in FE software ABAQUS. The geometric parameters of the RVE are given in fig. 2. The regular FE mesh of the model consist CPS4R, 4-noded, bilinear plane stress quadrilateral element with linear base functions with hourglass control. Most number of elements (27 348) and nodes (27856) has variant 3. The problem was solved in 2000 cycles with time step 2.5×10^{-10} s in the model.

Boundary conditions, FE mesh are described in fig 2a and in fig. 2b is described the mesh of 14 fibers. Dimensions are the same as for RVE with 6 fibers. The pressure load is applied on the upper side of RVE. The bottom side of RVE is fixed in the Y-direction and axis symmetry was applied on the both vertical sides. Calculations were made for following 4 variants:

- Variant 0 - model without fibers.
- Variant 1 - model with fiber radius $r_f = 1$ mm and volume fraction of fiber $v_f = 35\%$.
- Variant 2 - model with $r_f = 0.5$ mm and $v_f = 17,5\%$.
- Variant 3 - model with $r_f = 0.5$ mm and $v_f = 35\%$.

Tab. 1: Coordinates of investigated points

Point:	1	2	3	4	5	6	7	8	9	10	11	12	13	14	15
X[mm]	0	0	0	0	0	1.5	1.5	1.5	1.5	1.5	3	3	3	3	3
Y[mm]	6	3	0	-3	-6	6	3	0	-3	-6	6	3	0	-3	-6

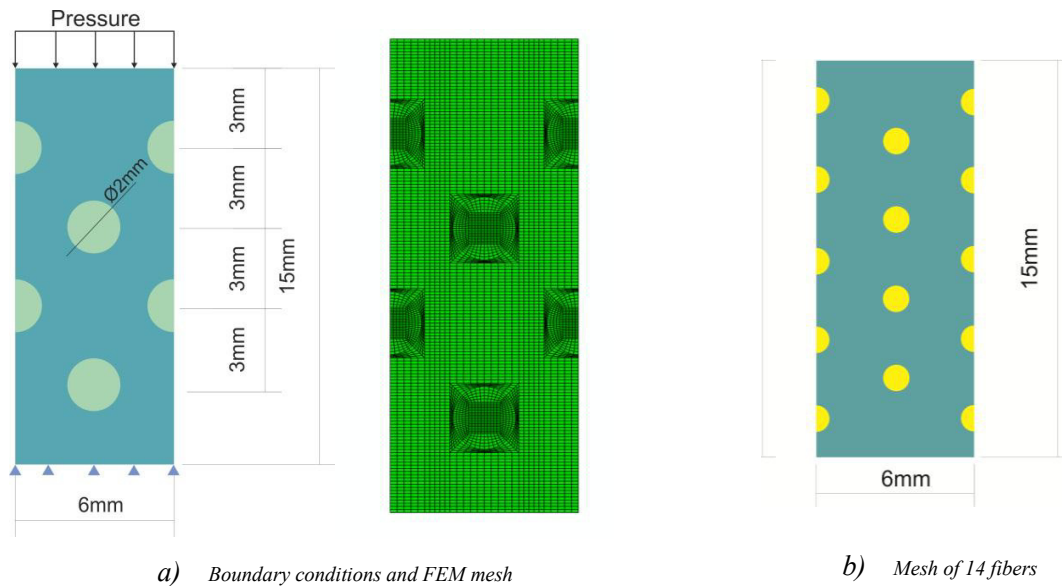
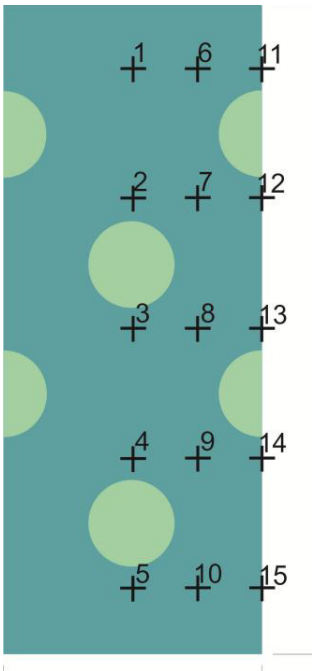
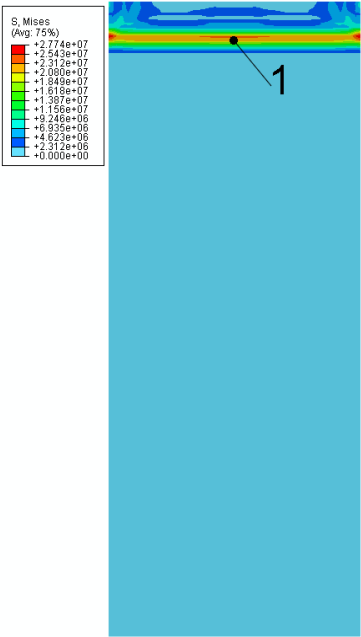


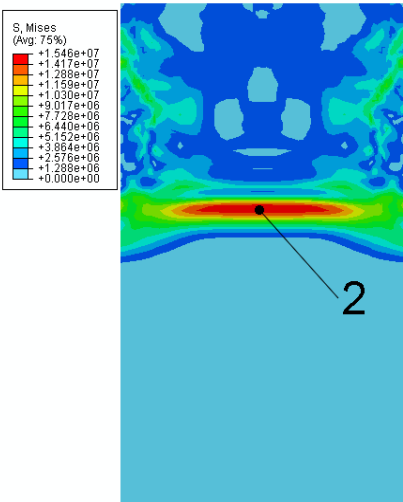
Fig. 2 Problem definition and boundary conditions



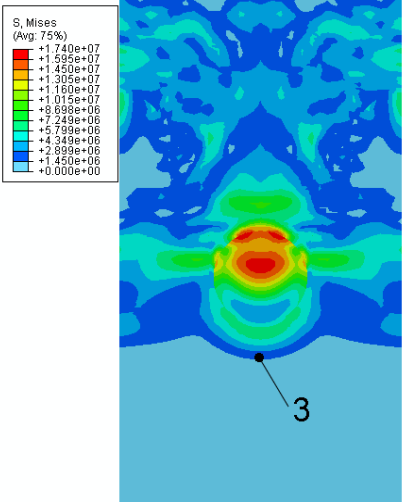
(a) valuated points



(b) Point 1, $t = 2.3275 \text{ E-}07 \text{ s}$



(c) Point 2, $t = 8.4774 \text{ E-}07 \text{ s}$



(d) Point 3, $t = 1.1477 \text{ E-}06 \text{ s}$

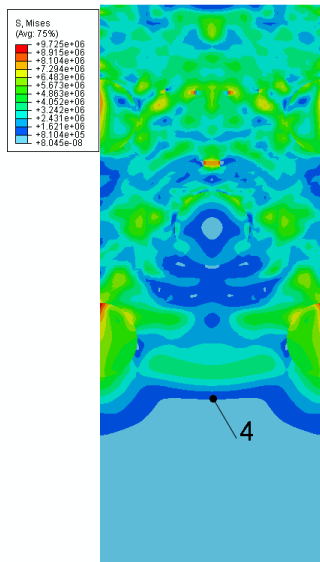
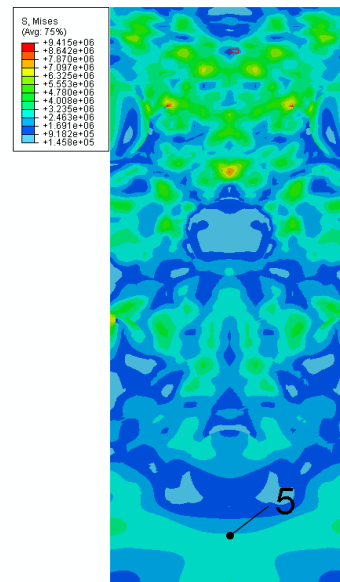
(e) Point 4, $t = 2.6301 \text{ E-}06 \text{ s}$ (f) Point 5, $t = 2.81165 \text{ E-}06$

Fig. 3 Von Mises stress in investigate points 1 to 5 for variant 1

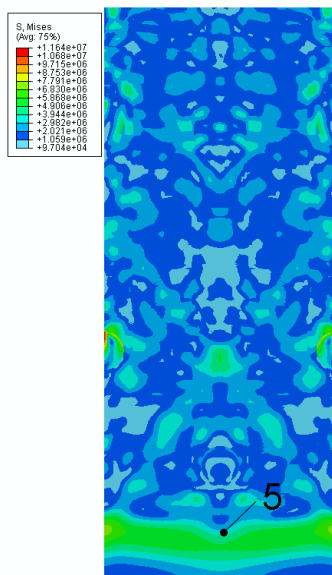
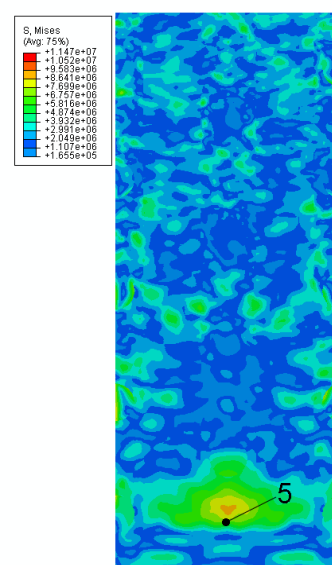
Variant 2, $t = 3.0227 \text{ E-}06$ Variant 3, $t = 3.005 \text{ E-}06$

Fig. 4 Von Mises stress in point 5

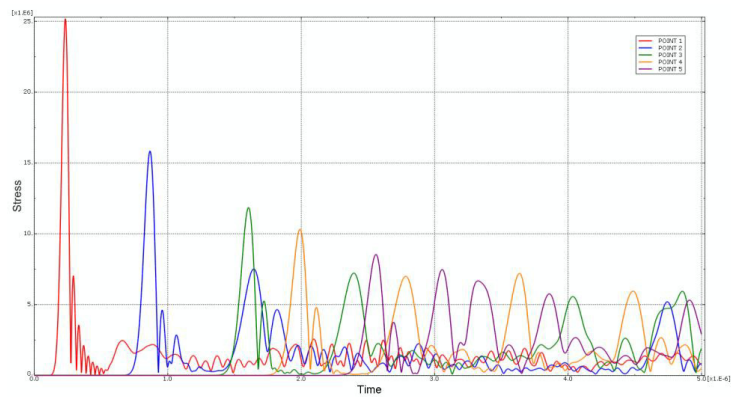


Fig. 5 Time course of the von Mises stress for variant 0

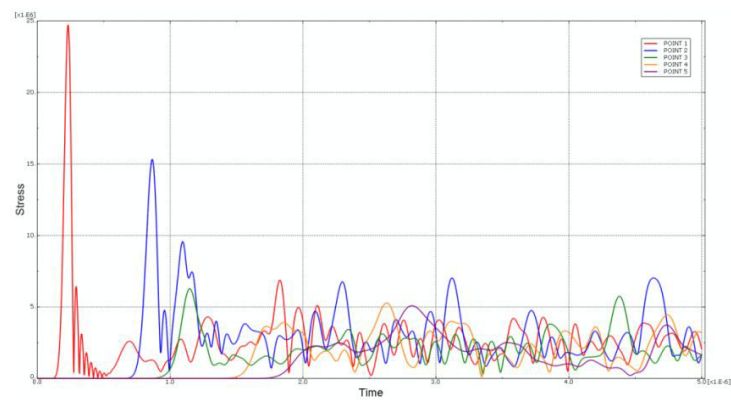


Fig. 6 Time course of the von Mises stress for variant 1

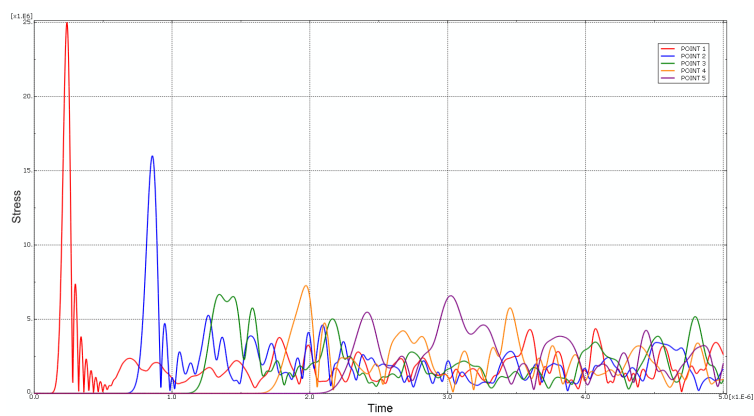


Fig. 7 Time course of the von Mises stress for variant 2

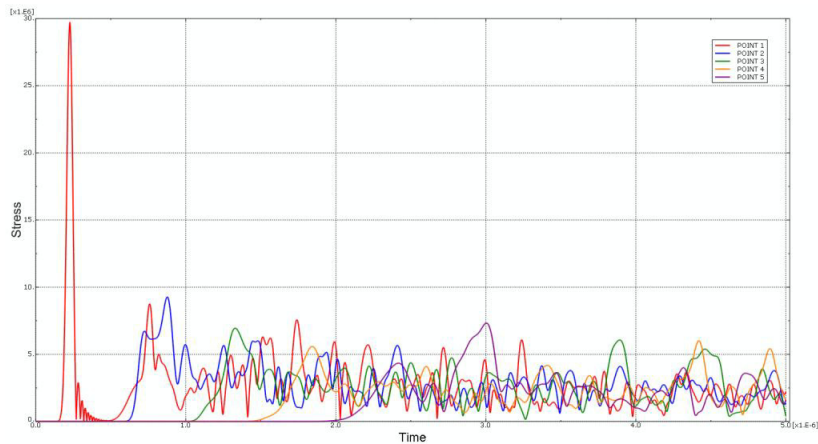


Fig. 8 Time course of the von Mises stress for variant 3

In fig. 3a are described coordinates of investigated points for given variants and in tab. 1 are their numerical values. At beginning the wave propagates parallel to the surface without any interaction (Fig.3b). After reaching first fibres the wave reflects from the fibre and interact with reflected part, however, the front of the wave is still expressive (Fig.3c). After the front of wave continues to propagate to lower part under the surface, the maximum in corresponding point is not as high as in many other points closer to the surface. Fig. 3e and fig.3f corresponds to the moment when the effective stress is maximal in point 5, but the stresses in points closer to the upper surface are larger because of complicated interactions of the waves. Fig. 4a and fig. 4b shows the same situation for variant 2 and variant 3. Fig.5 to fig.6 shows time course of the von Misses stresses after the shock achieving the surface of the material all in points 1 to 5. The red colour corresponds to the point 1 close to the surface and other colours to the other points below the first one. From the figures we can find the movement of the front as well the maximum of the stress in time. In fig.7 and fig.8 are described time courses of the von Mises stress for variant 2 and variant 3. If we define damping ratio as von Mises stress drop in 3 planes vertical to the upper surface defined by investigated points 1-5, 6-10 and 11-15 as

$$\text{Damping ratio} = \frac{(\sigma_{\text{von}})_i - (\sigma_{\text{von}})_{i-4}}{(\sigma_{\text{von}})_i}, \quad i = 5, 10, 15, \quad (10)$$

then damping ratios of stress waves for going through indicated planes are given in tab. 2. As expected, the largest value of damping ratio is for variant 3 in plane 11-15 and is 0.8591. This means that the drop of maximum von Mises stress is almost 86 percentage

Tab: 2 Damping ratios of stress waves

Plane	Variant 0	Variant 1	Variant 2	Variant3
1 - 5	0.6607	0.7938	0.7367	0.7535
6-10	0.6126	0.7969	0.7037	0.8049
11-15	0.6282	0.8519	0.6359	0.8591

We note that computational models do not contain any other damping except of the interaction of the shock wave with fibres (each material contains some imperfections in the structure and in material properties and so, there is some material damping also in homogeneous material) and shows as the reinforcing fibres because of very different material properties of both material components result in very efficient damping of shock waves and thus such composite can be very efficient in defence against explosion.

The shock wave in homogeneous material is not influenced by propagation through material and only when it is reflected on the boundaries there is an interaction with propagated wave [19, 20]. On the other side there is very complicated interaction of the wave by reflection, and refraction on the interface between softer matrix and stiffer fibres leading to strong damping of the shock wave.

4. Conclusion

The problem of shock wave propagation was studied in this work. Computational simulations were performed in FE software ABAQUS. The FEM simulation was based on the RVE model. Simulations are carried out with fibers with different diameters and volume fraction of fiber. The proposed procedure allow very effectively without expensive experiments to study the behaviour of composite materials from all points of view, the material structure topology, material properties of components, percentage of reinforcement, etc. That the longest calculation time was for variant 3 and used CPU time was only 1:47:17 on Pentium desktop computer with Intel core i5 with 2,6 GHz frequency and 8 GB RAM.

Acknowledgements

The authors gratefully acknowledge the support by the Slovak Grant Agency VEGA 1/1226/12 and Slovak and Technology Assistance Agency registered under number APVV-0736-12.

References

- [1] Š. Markuš., *Vibration Mechanics of Cylindrical Shells*, VEDA 1982, Bratislava (in Slovak).
- [2] T. Mazúch , *Semianalytical FE approach to modeling of the cylinders flexural vibration*, Building Research Journal, 52 (2005).
- [3] W. Ostachowicz, P. Kudelka., M. Krawczuk, A. Zak , *Guided waves in structures for SHM: The Time-domain Spectral Element Method*. JohnWiley & Sons, 2012.
- [4] R. Brepta, *Shock and waves in Solid Elastic Bodies*. Czech Technical University in Prague, 1977 (in Czech).
- [5] J. Sladek, P. Stanak, Z.D. Han, V. Sladek, S.N. Atluri, *Applications of the MLPG Method in Engineering & Sciences: Review*, CMES 5 (2013) 423-475.
- [6] M. Žmindák, D. Riecky, Z. Pelagić, M. Dudinsky, *Meshless local Petrov-Galerkin formulation for static analysis of composite plates reinforced by unidirectional fibers*. American Journal of Mechanical Engineering 2013.
- [7] S. Gopalakrishnan, A. Chakraborty, D.R. Mahapatra, *Spectral Finite Element Method*, Springer, 2008.
- [8] J.L. Humar, H. Xia, *Dynamic response analysis in the frequency domain*, Earthquake Engineering and Structural Dynamics, 22, (1993) 1-12.
- [9] L.E. Malvern, *Introduction to Mechanics of a Continuous Medium*, Prentice Hall, Englewood Cliffs, New Jersey, 1969.
- [10] H.C. Wu, *Continuum Mechanics and Plasticity*, Chapman and Hall/CRC London, 2005.
- [11] V. Kompiš, M. Vančo, V. Ferencey, *Shock waves propagation in composite materials*, Mechanical Engineering 61, (2010) 73-88.
- [12] K.J. Bathe, G. Noh, *Insight into an implicit time integration scheme for structural dynamics*, Computers and Structures, 98-99 (2012) 1 – 6.
- [13] S. Ham, K.J. Bathe, *A finite element method enriched for wave propagation problems*, Computers and Structures, 94-95 (2012), 1-12.
- [14] R. Kolman, S.S Cho, K.C. Park, *An explicit time integration algorithm for finite element computations of discontinuous wave propagation problems*, Dynamics of Machines, Prague, 2007 pp. 65 – 72.
- [15] M. Okrouhlik, *When a “Good agreement” is not enough*. In: Dynamics of solid and defomable bodies, Ústí n. L., Czech Republic, 2007.
- [16] J. Plešek, R. Kolman, D. Gabriel, *Estimation of the critical time step for explicit integration*. In: Engineering mechanics, 18-th International conference, Svratka, Czech Republic, 201, pp. 1001-1010.
- [17] M. Okrouhlik, *Computational Aspects of Stress Waves Problems in Solids – 2nd European Conference on Computational Mechanics*, Abstracts Vol. 1, Cracow, Poland, 2001, pp. 1- 30.
- [18] J. Trnka, T. Mazuch, *Experimental and theoretical analysis of wave propagation in cylindrical shells*. In: Engineering Mechanics, 2000, pp.277-281 (in Czech).
- [19] S.J. Hiermaier, *Structures Under Crash and Impact*, Continuum mechanics, discretization and experimental characterization, Springer, New York, 2008.
- [20] V. Kompiš, Z. Murčínková, S. Rjasanow, R. Grzibovskis, Q. Qing-Hua, *Computational simulation methods for fiber reinforced composites*. In: Frontiers of Architecture and Civil Engineering in China 4 (2010) 396-401.